

Mechanisms of unexpected reduction in hole concentration in Al-doped 4H-SiC by 200 keV electron irradiation

Hideharu Matsuura,^{1,a)} Nobumasa Minohara,¹ and Takeshi Ohshima²

¹Department of Electronic Engineering and Computer Science, Osaka Electro-Communication University, 18-8 Hatsu-cho, Neyagawa, Osaka 572-8530, Japan

²Japan Atomic Energy Agency, 1233 Watanuki, Takasaki, Gunma 370-1292, Japan

(Received 3 March 2008; accepted 17 June 2008; published online 25 August 2008)

The hole concentration in Al-doped *p*-type 4H-SiC was found to be significantly reduced by electron irradiation when compared to the hole concentration in Al-doped *p*-type Si; this is an unexpected result. The temperature dependence of the hole concentration $p(T)$ in Al-doped 4H-SiC irradiated with 200 keV electrons at various fluences was measured. Only substitutional C atoms in SiC can be displaced by irradiation with 200 keV electrons. The reduction in $p(T)$ by the electron irradiation was found to be mainly due to a decrease in Al acceptors and not due to an increase in defects (e.g., C vacancies) located around the middle of the bandgap in SiC. Based on the analysis of $p(T)$, two types of acceptor species were detected and the density and energy level of each acceptor species were determined. An equation describing the fluence dependence of each acceptor density is proposed. The results suggest that for the 200 keV electron irradiation, a substitutional C atom bonded to an Al acceptor was more easily displaced than a substitutional C atom bonded to four Si atoms. © 2008 American Institute of Physics. [DOI: 10.1063/1.2969788]

I. INTRODUCTION

SiC is a wide bandgap semiconductor with significant potential for applications in high power and high frequency devices capable of operation at elevated temperatures. For electrons with energies greater than 0.5 MeV, minority-carrier-lifetime degradation by electron irradiation in SiC was reported to be lower than that in GaAs by more than three orders of magnitude and lower than that in Si by at least one order of magnitude.¹ This indicates the greatly superior resistance of SiC to displacement damage in radiation environments.

Electron irradiation is an excellent tool for the controlled generation of intrinsic defects in Si for use in high power devices.² On the other hand, electron irradiation degrades the conversion efficiency of Si solar cells, for example, such as those used in space applications.³⁻⁶ Therefore, electron-radiation damage in Si has been intensively investigated in the past. On the other hand, ion-implantation-induced defects in 4H-SiC epitaxial layers have been reported.^{7,8} However, the understanding of electron-radiation damage in SiC is far from complete.

By comparing electron-radiation damage in 4H-SiC with that in Si,^{6,9,10} it was found that the reduction in the temperature-dependent hole concentration $p(T)$ in Al-doped *p*-type 4H-SiC by electron irradiation was much larger than in Al-doped *p*-type Si, as shown in Fig. 1, even though the electron energy (0.5 MeV) and fluence ($0.5 \times 10^{15} \text{ cm}^{-2}$) used for SiC were less than those used for Si (1 MeV and $1 \times 10^{16} \text{ cm}^{-2}$). The reduction in $p(T)$ in B-doped or Ga-doped *p*-type Si was found to be similar to that in Al-doped Si.⁶ Moreover, $p(T)$ in Al-doped 4H-SiC irradiated with a $1 \times 10^{16} \text{ cm}^{-2}$ fluence of 0.5 or 1 MeV electrons could not

be measured because of the much higher resistivity of the irradiated samples.¹⁰ Since the large reduction in $p(T)$ in Al-doped 4H-SiC by the electron irradiation was an unexpected result, the reduction in $p(T)$ by irradiation with different electron energies was investigated.⁹⁻¹¹

The densities and energy levels of traps have usually been evaluated using deep-level transient spectroscopy (DLTS). However, a quantitative relationship between $p(T)$ and trap densities cannot be obtained using DLTS. The reason for this is that in the DLTS analysis, the following approximation is assumed:^{12,13}

$$C(t) = C(\infty) \sqrt{1 - \frac{N_t}{N_d + N_t} \exp\left(-\frac{t}{\tau_t}\right)} \approx C(\infty) \left[1 - \frac{N_t}{2(N_d + N_t)} \exp\left(-\frac{t}{\tau_t}\right) \right] \quad (1)$$

when

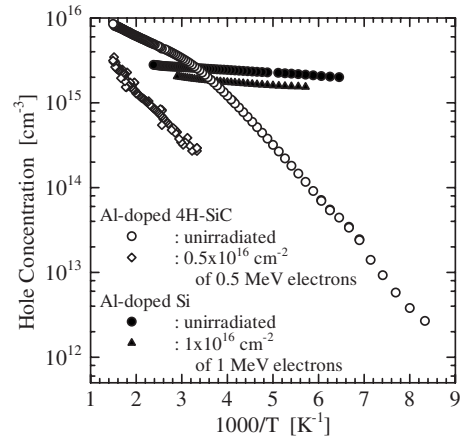


FIG. 1. Temperature dependence of hole concentration for Al-doped 4H-SiC and Si before and after electron irradiation.

^{a)}Electronic mail: matsuura@isc.osakac.ac.jp.

$$\frac{N_t}{N_d + N_t} \ll 1, \quad (2)$$

where $C(t)$ is the capacitance transient after removal of the filling pulse and return to the steady-state reverse bias voltage in the DLTS measurement sequence, $C(\infty)$ is the steady-state capacitance, N_d is the dopant density (i.e., donor or acceptor density), N_t is the trap density, and τ_t is the time constant corresponding to the trap. Based on Eq. (2), DLTS can determine the density and energy level of the trap only when N_t is much lower than N_d , indicating that the trap determined by DLTS barely affects $p(T)$. Moreover, transient capacitance methods (e.g., DLTS and isothermal capacitance transient spectroscopy) cannot be applied to high-resistivity semiconductors such as heavily irradiated semiconductors because the measured capacitance of a diode is determined by the thickness of the diode, not by the depletion region of the junction due to its long dielectric relaxation time.^{14–19}

If the densities and energy levels of traps can be determined using experimental $p(T)$ values, the relationship between $p(T)$ and trap densities can be investigated directly. For the analysis of $p(T)$, a graphical peak analysis method [free carrier concentration spectroscopy (FCCS)] has been proposed and tested,^{20–26} which can determine the densities and energy levels of acceptors and hole traps from experimental $p(T)$ values without any assumptions regarding acceptor species or hole traps.

Since the atomic mass of C is smaller than that of Si, the maximum energy transferred from an electron to one substitutional C atom (C_s) in SiC by elastic collision is larger than the energy transferred to one substitutional Si atom (Si_s). This indicates that the minimum electron energy necessary for displacing C_s should be lower than that for Si_s . According to experimental and theoretical considerations,^{1,10,27,28} 200 keV electrons can only displace C_s in SiC. Therefore, we have investigated the reduction in $p(T)$ in Al-doped p -type 4H-SiC by the irradiation of 200 keV electrons at several fluences.

II. EXPERIMENTAL

A 10- μm -thick Al-doped p -type 4H-SiC epilayer on n -type 4H-SiC (thickness: 376 μm , with a resistivity of 0.02 $\Omega\text{ cm}$) was cut to a size of $1 \times 1\text{ cm}^2$, forming a sample. $p(T)$ and the temperature dependence of the hole mobility $\mu_h(T)$ were obtained by Hall-effect measurements, in the van der Pauw configuration, within the temperature range of 120–650 K in a 1.4 T magnetic field. $p(T)$ and $\mu_h(T)$ were measured before irradiation, and then the sample was irradiated with 200 keV electrons with a fluence of $1 \times 10^{16}\text{ cm}^{-2}$. After the Hall-effect measurements were carried out, the sample was again irradiated but now with a fluence of $2 \times 10^{16}\text{ cm}^{-2}$. The Hall-effect measurement and irradiation with the $2 \times 10^{16}\text{ cm}^{-2}$ fluence of 200 keV electrons were repeated. Consequently, $p(T)$ and $\mu_h(T)$ for the samples irradiated with total fluences (Φ) of 0, 1×10^{16} , 3×10^{16} , 5×10^{16} , 7×10^{16} , and $9 \times 10^{16}\text{ cm}^{-2}$ were measured. Although the Hall-effect measurements were carried

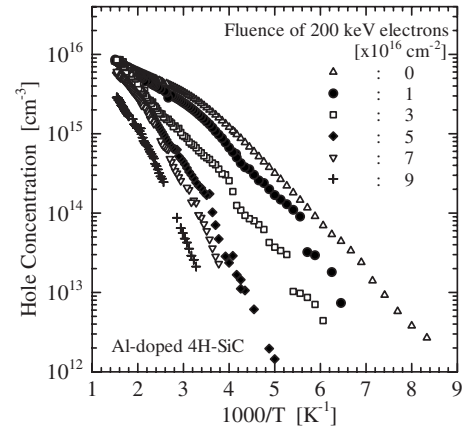


FIG. 2. Temperature dependence of hole concentration for Al-doped 4H-SiC before and after irradiation with 200 keV electrons at five different fluences.

out twice for each fluence, $p(T)$ remained unchanged, indicating that any defects affecting $p(T)$ were not annealed for measurement temperature lower than 650 K.

The densities and energy levels of acceptors and hole traps were determined by FCCS from the $p(T)$ values. Using the experimental $p(T)$, the FCCS signal is defined as^{20–26}

$$H(T, E_{\text{ref}}) \equiv \frac{p(T)^2}{(kT)^{5/2}} \exp\left(\frac{E_{\text{ref}}}{kT}\right), \quad (3)$$

where k is the Boltzmann constant and E_{ref} is the parameter that can shift the peak temperature of the FCCS signal within the temperature range of the measurement. The FCCS signal has a peak at the temperature corresponding to each acceptor level or hole-trap level. From each peak, the density and energy level of the corresponding acceptor or hole trap can be accurately determined. The application software for FCCS (for the Windows operating system) can be downloaded for free at our Web site (<http://www.osakac.ac.jp/labs/matsuura/>).

III. RESULTS AND DISCUSSION

A. Reduction in $p(T)$ by irradiation with 200 keV electrons

Figure 2 shows the experimental $p(T)$ for fluences of 0, 1×10^{16} , 3×10^{16} , 5×10^{16} , 7×10^{16} , and $9 \times 10^{16}\text{ cm}^{-2}$ denoted by open triangles, solid circles, open squares, solid diamonds, open inverse triangles, and crosses, respectively. Judging from the magnitude of $\mu_h(T)$, band conduction of holes was dominant in these samples within the temperature range of the measurement. The $p(T)$ at low temperatures decreased significantly with increasing Φ , whereas the $p(T)$ at high temperatures was changed slightly by the irradiation.

B. Reduction in $p(T)$ by creation of deep defects

200 keV electrons can only displace C_s . Therefore, a C vacancy (V_C) and an interstitial C (C_i) are created by irradiation. When the rate of displacement of C_s by collision with a 200 keV electron is denoted by κ_{CD} , the density $N_{\text{CD}}(\Phi)$ of the carbon-related defect (V_C or C_i) can be expressed as

$$\frac{dN_{CD}(\Phi)}{d\Phi} = \kappa_{CD}. \quad (4)$$

Therefore,

$$N_{CD}(\Phi) = \kappa_{CD}\Phi. \quad (5)$$

In other words, κ_{CD} is the generation rate of the carbon-related defect. The densities of defects related to C_s displacement (i.e., $Z_{1/2}$ center with $E_C - 0.65$ eV and $EH_{6/7}$ center with $E_C - 1.55$ eV) were reported to be nearly proportional to Φ ,²⁹ which is expected from Eq. (5), where E_C is the conduction band minimum. The HK4 center with $E_V + 1.44$ eV was reported to be a complex including defects induced by the C_s displacement,²⁹ where E_V is the valence band maximum. According to studies on intrinsic defects in SiC,³⁰ the (0/+) level of V_C is at $E_V + 1.4$ eV and its (+/+ +) level is at $E_V + 1.68$ eV. Since the defects induced by C_s displacement are located around the middle of the bandgap in SiC, they should act as hole traps.

We can consider the influence of $N_{CD}(\Phi)$ on $p(T)$. Using the $p(T)$ for the unirradiated sample in Fig. 2, the acceptor densities and acceptor levels before irradiation were determined by FCCS. The density (N_{Al}) and energy level (E_{Al}) of the shallow acceptor were $5.3 \times 10^{15} \text{ cm}^{-3}$ and $E_V + 0.20$ eV, respectively, while the density (N_{DA}) and energy level (E_{DA}) of the deep acceptor (or hole trap) were $3.7 \times 10^{15} \text{ cm}^{-3}$ and $E_V + 0.37$ eV, respectively. Moreover, the compensating density (N_{comp}), which is the sum of the densities of donors and hole traps deeper than E_{DA} , was $2 \times 10^{13} \text{ cm}^{-3}$.

Because the energy level of an Al acceptor in 4H-SiC was reported to be approximately $E_V + 0.2$ eV, from photoluminescence³¹ and Hall-effect³² measurements, the shallow acceptor detected here is assigned to an Al acceptor. Although the energy level of a B acceptor in 4H-SiC was reported to be approximately $E_V + 0.3$ eV,³² the concentration of B atoms in the 4H-SiC epilayer was less than $4 \times 10^{14} \text{ cm}^{-3}$ as determined by secondary ion mass spectroscopy. Therefore, the deep acceptor detected here is not a B acceptor.

$p(T)$ was numerically simulated using the following two equations:

$$p(T) + N_{comp} = N_{Al}f_{FD}(E_{Al}) + N_{DA}f_{FD}(E_{DA}) \quad (6)$$

and

$$p(T) = N_V(T) \exp\left[-\frac{E_F(T) - E_V}{kT}\right], \quad (7)$$

where $f_{FD}(E)$ is the Fermi–Dirac distribution function that is given by

$$f_{FD}(E) = \frac{1}{1 + 4 \exp\left[\frac{E - E_F(T)}{kT}\right]}, \quad (8)$$

$N_V(T)$ is the effective density of states in the valence band, described as

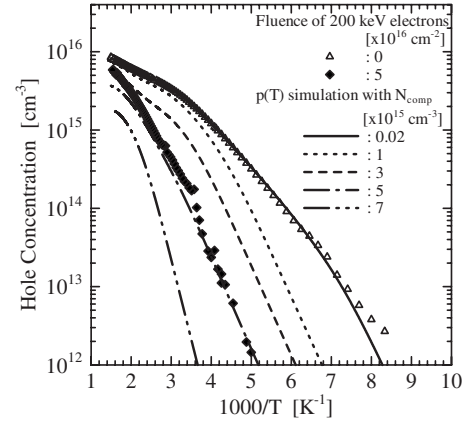


FIG. 3. Comparison of experimental $p(T)$ with $p(T)$ simulations using several N_{comp} .

$$N_V(T) = 2 \left(\frac{2\pi m_h^* kT}{h^2} \right)^{3/2}, \quad (9)$$

$E_F(T)$ is the Fermi level, m_h^* is the hole effective mass, and h is Planck's constant.

In Fig. 3, the open triangles represent $p(T)$ for the unirradiated case and the solid line is the $p(T)$ simulation with N_{Al} of $5.3 \times 10^{15} \text{ cm}^{-3}$, E_{Al} of $E_V + 0.20$ eV, N_{DA} of $3.7 \times 10^{15} \text{ cm}^{-3}$, E_{DA} of $E_V + 0.37$ eV, and N_{comp} of $2 \times 10^{13} \text{ cm}^{-3}$. Since the $p(T)$ simulation (solid line) is in good agreement with the experimental $p(T)$ (open triangles) for the unirradiated case, the values obtained by FCCS are reliable.

In order to simulate $p(T)$ for the irradiated case, the following is assumed: (1) The 200 keV electron irradiation does not change the densities and energy levels of the acceptors, and (2) the irradiation only increases N_{comp} , that is, the sum of the N_{comp} for the unirradiated case and $N_{CD}(\Phi)$, which was increased by the irradiation. Figure 3 also shows the experimental $p(T)$ (solid diamonds) for the $5 \times 10^{16} \text{ cm}^{-2}$ fluence and the $p(T)$ simulations with N_{comp} of 1×10^{15} , 3×10^{15} , 5×10^{15} , and $7 \times 10^{15} \text{ cm}^{-3}$ denoted by dotted, broken, dashed-dotted, and dashed double-dotted lines, respectively.

As is clear from Fig. 3, the $p(T)$ simulation over the whole temperature range decreased with increasing N_{comp} . On the other hand, the experimental $p(T)$ at low temperatures decreased significantly with increasing Φ , whereas the $p(T)$ at high temperatures was slightly changed by the irradiation. For example, the solid diamonds at low temperatures are close to the $p(T)$ simulation (dashed-dotted line) with N_{comp} of $5 \times 10^{15} \text{ cm}^{-3}$, while at high temperatures they are higher than the dashed-dotted line. Judging from the above discussion, the reduction in $p(T)$ by the electron irradiation could not be explained just by the increase in densities of the deep defects.

C. Fluence dependence of acceptor densities and hole-trap densities

The densities and energy levels of acceptors and N_{comp} were determined by FCCS using the experimental $p(T)$ shown in Fig. 2, as listed in Table I. At fluences of $\leq 7 \times 10^{16} \text{ cm}^{-2}$, two types of acceptor species were detected:

TABLE I. Results obtained by FCCS in Al-doped 4H-SiC irradiated by 200 keV electrons.

Fluence ($\times 10^{16}$ cm $^{-2}$)	0	1	3	5	7	9	Origins
$E_{\text{Al}} - E_{\text{V}}$ (eV)	0.20	0.22	0.23	0.23	0.23	...	Al acceptor
N_{Al} ($\times 10^{15}$ cm $^{-3}$)	5.3	4.3	1.4	0.5	0.3	<0.1	
$E_{\text{DA}} - E_{\text{V}}$ (eV)	0.37	0.37	0.38	0.38	0.39	0.39	?
N_{DA} ($\times 10^{15}$ cm $^{-3}$)	3.7	5.4	11	6.9	7.6	2.4	
N_{comp} ($\times 10^{15}$ cm $^{-3}$)	0.02	0.09	0.16	0.30	0.35	0.40	Deeper hole traps and donors

One acceptor level was approximately $E_{\text{V}} + 0.22$ eV, while the other acceptor level was approximately $E_{\text{V}} + 0.38$ eV. The former acceptor species is assigned to an Al acceptor, while the latter acceptor species has not been assigned. At a fluence of 9×10^{16} cm $^{-2}$, only the deep acceptor was detected because N_{Al} was much lower than N_{DA} . Figure 4 depicts the fluence dependence of N_{Al} and N_{DA} . N_{Al} decreased with increasing Φ , and finally there are no more Al acceptors. On the other hand, N_{DA} initially increased with Φ and then decreased.

In order to reduce N_{Al} by the 200 keV electron irradiation, the surroundings of the Al acceptor need to be changed by C_{s} displacement since the Al acceptor is an Al atom (Al_{Si}) located at a Si sublattice and bonded to four C_{s} . This indicates that the rate of decrease in N_{Al} by the irradiation is proportional to N_{Al} . Consequently, the differential equation that leads to fluence dependence of Al acceptors $N_{\text{Al}}(\Phi)$ is given by

$$\frac{dN_{\text{Al}}(\Phi)}{d\Phi} = -\kappa_{\text{Al}}N_{\text{Al}}(\Phi), \quad (10)$$

where κ_{Al} is the removal coefficient (or removal cross section) of Al acceptors for 200 keV electron irradiation. Therefore,

$$N_{\text{Al}}(\Phi) = N_{\text{Al}}(0)\exp(-\kappa_{\text{Al}}\Phi). \quad (11)$$

Figure 5 shows $N_{\text{Al}}(\Phi)$ in a semilogarithmic scale, and the solid line is a straight line obtained by least-squares fitting. Since the straight line is in good agreement with the solid circles in the semilogarithmic plots, Eq. (11) is applicable for the fluence dependence of N_{Al} . κ_{Al} is then determined from the slope as 4.4×10^{-17} cm 2 . Since by irradiation

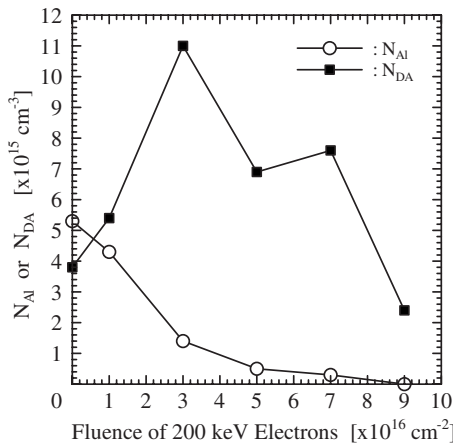


FIG. 4. Fluence dependence of shallow or deep acceptor density.

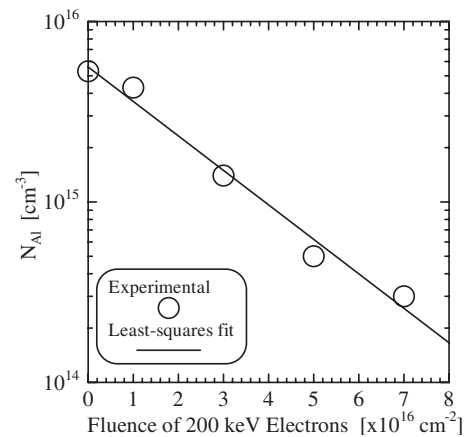
of 1 MeV electrons the removal coefficient of B acceptors in p -type Si with a B-doping concentration of 2×10^{16} cm $^{-3}$ was reported to be approximately 8×10^{-18} cm 2 ,⁶ the electron-radiation resistance of p -type 4H-SiC is inferior to that of p -type Si.

In Fig. 4, at fluences of $\leq 3 \times 10^{16}$ cm $^{-2}$, N_{DA} increased with increasing Φ , while N_{Al} decreased. Furthermore, the increment in N_{DA} is close to the decrement in N_{Al} . This experimental result may indicate that the 200 keV electron irradiation transforms the Al acceptor into the deep acceptor. On the other hand, N_{DA} is assumed to be decreased by the change in the surroundings of the deep acceptor due to C_{s} displacement. As a result, the differential equation describing the fluence dependence of the deep acceptor density $N_{\text{DA}}(\Phi)$ can be expressed as

$$\frac{dN_{\text{DA}}(\Phi)}{d\Phi} = -\frac{dN_{\text{Al}}(\Phi)}{d\Phi} - \kappa_{\text{DA}}N_{\text{DA}}(\Phi), \quad (12)$$

where κ_{DA} is the removal coefficient (or removal cross section) of the deep acceptors for 200 keV electron irradiation. Figure 6 depicts the experimental fluence dependence of N_{DA} and the simulated $N_{\text{DA}}(\Phi)$ with κ_{DA} of 1.0×10^{-17} cm 2 using Eq. (12), denoted by solid squares and the solid line, respectively. The simulation results in Fig. 6 show qualitative agreement with the experimental data but not quantitative agreement.

In Table I, it can be seen that N_{comp} is increased slightly with increasing Φ ; however, it is less than 10^{15} cm $^{-3}$. This might be because V_{C} is increased by C_{s} displacement. Consequently, the reduction in $p(T)$ by the 200 keV electron irradiation is mainly due to the decrease in N_{Al} , not to the increase in the density of V_{C} .

FIG. 5. Dependence of N_{Al} on the fluence of 200 keV electrons.

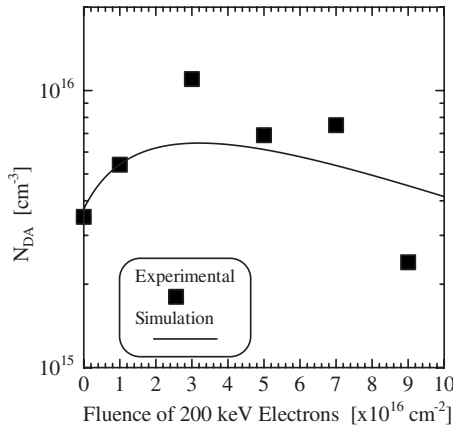


FIG. 6. Comparison between experimental and simulated $N_{DA}(\Phi)$.

D. Possible mechanisms of reduction in $p(T)$ by 200 keV electron irradiation

The following findings have been obtained from the study of 200 keV electron irradiation in Al-doped p -type 4H-SiC: (1) The reduction in $p(T)$ is greater than expected from the increase in V_C , (2) the reduction in $p(T)$ is mainly due to the decrease in N_{Al} , and (3) Al acceptors can be transformed into the deep acceptors with $E_V+0.38$ eV. On the other hand, the deep acceptor is most likely related to Al because the empirical relationship between N_{Al} and N_{DA} in unirradiated Al-doped p -type 4H-SiC epilayers was reported to be^{10,22}

$$N_{DA} = 0.6N_{Al}. \quad (13)$$

Therefore, Eq. (11) indicates that one of the four C_s bonded to one Al_{Si} is displaced by the irradiation, and the Al_{Si} then cannot act as an acceptor with $E_V+0.2$ eV (i.e., Al acceptor). Moreover, Eq. (12) suggests that N_{DA} is increased when there are abundant Al acceptors because the irradiation transforms the Al acceptor into the deep acceptor, while N_{DA} is decreased when there is a shortage of Al acceptors.

Judging from the above discussion, the deep acceptor with $E_V+0.38$ eV might be a complex ($Al_{Si}-V_C$) of Al_{Si} and V_C . By irradiation, N_{DA} is increased by the displacement of one of the four C_s bonded to an Al_{Si} by the irradiation, while N_{DA} is decreased by the displacement of one of the three C_s bonded to an $Al_{Si}-V_C$.

B atoms in 4H-SiC were reported to form two electrical levels in the lower half of the bandgap.³³ One is located at approximately $E_V+0.3$ eV, as determined by Hall-effect measurements,³³ while the other is between $E_V+0.55$ and 0.65 eV, as determined by DLTS.³⁴ The shallow level is assigned to a B acceptor (B_{Si}) at a Si sublattice. The probable identification of the deep level is a complex ($B_{Si}-V_C$) of the B_{Si} and its nearest neighbor V_C .^{35,36} In analogy with B in B-doped 4H-SiC, the deep acceptor in Al-doped 4H-SiC may be an $Al_{Si}-V_C$ complex, which has been detected by electron paramagnetic resonance spectroscopy.³⁶ From theoretical calculations,³⁷ on the other hand, $Al_{Si}-V_C$ was reported to be located around the middle of the bandgap in 4H-SiC, not at $E_V+0.38$ eV.

The 200 keV electron irradiation initially creates V_C and C_i in SiC matrix. Compared to V_C , C_i is rather mobile but can migrate and react with other defects or impurities and form more stable defect complexes.³⁸ When C_i reacts with the Al acceptor and forms a defect complex, the Al atom does not act as the acceptor with $E_V+0.2$ eV and the complex might behave as the acceptor with $E_V+0.38$ eV. This process can be also expressed as Eq. (10). In this case, the increment in V_C created by the irradiation should be greater than or equal to the decrement in the Al acceptors. Based on the discussion in Sec. III B, however, the increment in deep levels such as V_C is much less than the decrement in the Al acceptors. This indicates that by 200 keV electron irradiation, C_s bonded to the Al acceptor is likely displaced more easily than C_s bonded to four Si_s .

On the other hand, there is the possibility that almost all C_i created from Al-C bonds by irradiation may form complexes such as $Al-V_C-C_i$, which is assumed to obey Eq. (10). Although we obtained the quantitative fluence dependence of N_{Al} and the qualitative fluence dependence of N_{DA} and found that the 200 keV electron irradiation transforms the Al acceptor into the deep acceptor, we have no evidence of the origin of the deep acceptor to date. In order to identify the deep acceptor with approximately $E_V+0.38$ eV in Al-doped p -type 4H-SiC, therefore, further research is required.

IV. CONCLUSIONS

In Al-doped p -type 4H-SiC epilayers, the dependence of $p(T)$ on the fluence of 200 keV electrons was measured. In the analysis of $p(T)$, the reduction in $p(T)$ by the 200 keV electron irradiation was mainly due to the decrease in Al acceptors and not due to the increase in C vacancies. Moreover, a differential equation describing the fluence dependence on the density of the Al acceptors or the deep acceptors was proposed. Although the decrease in Al acceptors and the increase in C vacancies were due to the displacement of substitutional C atoms by the 200 keV electron irradiation, the decrease in the Al acceptor density was much greater than the increase in the C vacancy density. This suggests that the displacement of C bonded to the Al acceptor occurred much more easily than that of C bonded to four Si atoms.

ACKNOWLEDGMENTS

This work was partially supported by the Academic Frontier Promotion Projects of the Ministry of Education, Culture, Sports, Science and Technology of Japan in 1998–2002 and 2003–2007, and partially supported by a Grant-in-Aid for Scientific Research (C) of the Japan Society for the Promotion of Science in 2006 and 2007 (Grant No. 18560356).

¹A. L. Barry, B. Lehman, D. Fritsch, and D. Bräuning, *IEEE Trans. Nucl. Sci.* **38**, 1111 (1991).

²S. M. Sze, *Physics of Semiconductor Devices*, 2nd ed. (Wiley, New York, 1981), pp. 38 and 214.

³T. Hisamatsu, O. Kawasaki, S. Matsuda, T. Nakao, and Y. Wakow, *Sol. Energy Mater. Sol. Cells* **50**, 331 (1998).

⁴H. Matsuura, Y. Uchida, T. Hisamatsu, and S. Matsuda, *Jpn. J. Appl. Phys., Part 1* **37**, 6034 (1998).

⁵H. Matsuura, Y. Uchida, N. Nagai, T. Hisamatsu, T. Aburaya, and S.

- Matsuda, *Appl. Phys. Lett.* **76**, 2092 (2000).
- ⁶H. Matsuura, H. Iwata, S. Kagamihara, R. Ishihara, M. Komeda, H. Imai, M. Kikuta, Y. Inoue, T. Hisamatsu, S. Kawakita, T. Ohshima, and H. Itoh, *Jpn. J. Appl. Phys., Part 1* **45**, 2648 (2006).
- ⁷A. Hallén, A. Henry, P. Pellegrino, B. G. Svensson, and D. Åberg, *Mater. Sci. Eng., B* **61–62**, 378 (1999).
- ⁸D. Åberg, A. Hallén, P. Pellegrino, and B. G. Svensson, *Appl. Phys. Lett.* **78**, 2908 (2001).
- ⁹H. Matsuura, K. Aso, S. Kagamihara, H. Iwata, T. Ishida, and K. Nishikawa, *Appl. Phys. Lett.* **83**, 4981 (2003).
- ¹⁰H. Matsuura, S. Kagamihara, Y. Itoh, T. Ohshima, and H. Itoh, *Physica B (Amsterdam)* **376–377**, 342 (2006).
- ¹¹H. Matsuura, N. Minohara, Y. Inagawa, M. Takahashi, T. Ohshima, and H. Itoh, *Mater. Sci. Forum* **556–557**, 379 (2007).
- ¹²D. V. Lang, *J. Appl. Phys.* **45**, 3023 (1974).
- ¹³D. K. Schroder, *Semiconductor Materials and Device Characterization*, 2nd ed. (Wiley, New York, 1998), pp. 276 and 290.
- ¹⁴H. Matsuura, T. Okuno, H. Okushi, and K. Tanaka, *J. Appl. Phys.* **55**, 1012 (1984).
- ¹⁵H. Matsuura, *J. Appl. Phys.* **64**, 1964 (1988).
- ¹⁶H. Matsuura, *IEEE Trans. Electron Devices* **36**, 2908 (1989).
- ¹⁷H. Matsuura, in *Glow-Discharge Hydrogenated Amorphous Silicon*, edited by K. Tanaka (KTK Scientific, Tokyo, 1989), Chap. 10.
- ¹⁸H. Matsuura, *J. Appl. Phys.* **68**, 1138 (1990).
- ¹⁹H. Matsuura and H. Okushi, in *Amorphous and Micro-Crystalline Semiconductor Devices*, Materials and Device Physics Vol. II, edited by J. Kanicki (Artech House, Boston, 1992), Chap. 11.
- ²⁰H. Matsuura, Y. Masuda, Y. Chen, and S. Nishino, *Jpn. J. Appl. Phys., Part 1* **39**, 5069 (2000).
- ²¹H. Matsuura, K. Morita, K. Nishikawa, T. Mizukoshi, M. Segawa, and W. Susaki, *Jpn. J. Appl. Phys., Part 1* **41**, 496 (2002).
- ²²H. Matsuura, M. Komeda, S. Kagamihara, H. Iwata, R. Ishihara, T. Hatakeyama, T. Watanabe, K. Kojima, T. Shinohe, and K. Arai, *J. Appl. Phys.* **96**, 2708 (2004).
- ²³S. Kagamihara, H. Matsuura, T. Hatakeyama, T. Watanabe, M. Kushibe, T. Shinohe, and K. Arai, *J. Appl. Phys.* **96**, 5601 (2004).
- ²⁴H. Matsuura, H. Nagasawa, K. Yagi, and T. Kawahara, *J. Appl. Phys.* **96**, 7346 (2004).
- ²⁵H. Matsuura and K. Nishikawa, *J. Appl. Phys.* **97**, 093711 (2005).
- ²⁶H. Matsuura, *J. Mater. Sci.: Mater. Electron.* **19**, 720 (2008).
- ²⁷H. J. von Bardeleben, J. L. Cantin, L. Henry, and M. F. Barthe, *Phys. Rev. B* **62**, 10841 (2000).
- ²⁸L. Storasta, J. P. Bergman, E. Janzén, A. Henry, and J. Lu, *J. Appl. Phys.* **96**, 4909 (2004).
- ²⁹K. Danno and T. Kimoto, *Mater. Sci. Forum* **556–557**, 331 (2007).
- ³⁰F. Bechstedt, J. Furthmüller, U. Grossner, and C. Raffy, in *Zero- and Two-Dimensional Native Defects*, Silicon Carbide, edited by W. J. Choyke, H. Matsunami, and G. Pensl (Springer, Berlin, 2004), p. 11.
- ³¹M. Ikeda, H. Matsunami, and T. Tanaka, *Phys. Rev. B* **22**, 2842 (1980).
- ³²T. Troffer, M. Schadt, T. Frank, H. Itoh, G. Pensl, J. Heindl, H. P. Strunk, and M. Maier, *Phys. Status Solidi A* **162**, 277 (1997).
- ³³C. M. Zetterling, in *Process Technology for Silicon Carbide Devices*, edited by C. M. Zetterling (INSPEC, London, 2002), p. 54.
- ³⁴A. Schöner, K. Rottner, and N. Nordell, in *III-Nitride, SiC and Diamond Materials for Electronic Devices*, MRS Symposia Proceedings No. 423 (Materials Research Society, Pittsburgh, 1996), p. 661.
- ³⁵A. Gali, P. Deák, R. P. Devaty, and W. J. Choyke, *Phys. Rev. B* **60**, 10620 (1999).
- ³⁶I. V. Ilyin, E. N. Mokhov, and P. G. Baranov, *Mater. Sci. Forum* **353–356**, 521 (2001).
- ³⁷T. Hornos, A. Gali, N. T. Son, and E. Janzén, *Mater. Sci. Forum* **556–557**, 445 (2007).
- ³⁸M. Bockstedte, A. Mattausch, and O. Pankratov, in *Defect Migration and Annealing Mechanisms*, Silicon Carbide, edited by W. J. Choyke, H. Matsunami, and G. Pensl (Springer, Berlin, 2004), p. 37.